The Journal of Immunology

Critical Role of Apoptotic Speck Protein Containing a Caspase Recruitment Domain (ASC) and NLRP3 in Causing Necrosis and ASC Speck Formation Induced by *Porphyromonas gingivalis* in Human Cells

Max Tze-Han Huang, Debra J. Taxman, Elizabeth A. Holley-Guthrie, Chris B. Moore, Stephen B. Willingham, Victoria Madden, Rebecca Keyser Parsons, Gerald L. Featherstone, Roland R. Arnold, Brian P. O'Connor and Jenny Pan-Yun Ting

J Immunol 2009; 182:2395-2404; ;
doi: 10.4049/jimmunol.0800909
http://www.jimmunol.org/content/182/4/2395

The Journal of Immunology is published twice each month by
The American Association of Immunologists, Inc.,
1451 Rockville Pike, Suite 650, Rockville, MD 20852

Print ISSN: 0022-1767 Online ISSN: 1550-6606.

Critical Role of Apoptotic Speck Protein Containing a Caspase Recruitment Domain (ASC) and NLRP3 in Causing Necrosis and ASC Speck Formation Induced by *Porphyromonas gingivalis* in Human Cells[1]

Max Tze-Han Huang,* Debra J. Taxman,* Elizabeth A. Holley-Guthrie,* Chris B. Moore,* Stephen B. Willingham,† Victoria Madden,‡ Rebecca Keyser Parsons,§ Gerald L. Featherstone,§ Roland R. Arnold,§ Brian P. O'Connor,* and Jenny Pan-Yun Ting[2]*

Periodontal disease is a chronic inflammatory disorder that leads to the destruction of tooth-supporting tissue and affects 10–20 million people in the U.S. alone. The oral pathogen *Porphyromonas gingivalis* causes inflammatory host response leading to periodontal and other secondary inflammatory diseases. To identify molecular components that control host response to *P. gingivalis* in humans, roles for the NLR (NBD-LRR) protein, NLRP3 (cryopyrin, NALP3), and its adaptor apoptotic speck protein containing a C-terminal caspase recruitment domain (ASC) were studied. *P. gingivalis* strain A7436 induces cell death in THP1 monocytic cells and in human primary peripheral blood macrophages. This process is ASC and NLRP3 dependent and can be replicated by *P. gingivalis* LPS and *Escherichia coli*. *P. gingivalis*-induced cell death is caspase and IL-1 independent and exhibits morphological features consistent with necrosis including loss of membrane integrity and release of cellular content. Intriguingly, *P. gingivalis*-induced cell death is accompanied by the formation of ASC aggregation specks, a process not previously described during microbial infection. ASC specks are observed in *P. gingivalis*-infected primary human mononuclear cells and are dependent on NLRP3. This work shows that *P. gingivalis* causes ASC- and NLRP3-dependent necrosis, accompanied by ASC speck formation. *The Journal of Immunology,* 2009, 182: 2395–2404.

Periodontal disease is an inflammatory disorder that ultimately leads to the destruction of tooth supporting tissue and affects 7–15% of the U.S. adult population (1). It is one of the most common chronic infections and has been linked to a variety of systemic diseases such as atherosclerosis and other coronary diseases (2). Understanding the host response orchestrated by bacteria is critical in deciphering periodontal disease pathogenesis and ultimately in the design of effective therapeutics. One of the most frequently isolated oral microorganisms in periodontal diseased tissue is *Porphyromonas gingivalis,* a Gram-negative anaerobic bacterium. During an infection, bacteria may directly activate a host cell-mediated host response via various bacterial products, with *P. gingivalis*-derived LPS being a prominent pathogen-associated molecule. Monocytes/macrophages present in the periodontal tissues of patients are major contributors of host response during periodontal diseases (3). In addition to monocytes/macrophages, other immune cell types such as keratinocytes, fibroblasts, dendritic cells, and endothelial cells also play a role in producing cytokines (4–6). Gingival crevicular fluid obtained from diseased tissues of patients with periodontal disease exhibited elevated levels of IL-1β, IL-8, and IL-10 cytokines (7). Furthermore, *P. gingivalis* LPS has been shown to be an agonist of the pathogen-associated molecular pattern receptors, TLR2 and TLR4 (8–13). In addition, other bacterial products such as fimbriae have been shown to induce host immunity via TLR2 (14, 15). TLR2 is also critical in *P. gingivalis*-induced alveolar bone loss in mice (16).

Recently, new proteins that are members of the nucleotide-binding domain (NLR,[3] leucine-rich repeat (LRR) or NBD-LRR) family (http://www.genenames.org/genefamily/nacht.html; Ref. 17) have been identified as important regulators of the host response to pathogens and their components. This family was previously named as the CATERPILLER (C-terminal caspase recruitment domain (CARD), transcription enhancer, R (purine)-binding, pyrin, lots of leucine repeat), NOD-LRR (nucleotide-binding oligomerization domain leucine-rich repeat containing), NOD-like receptor (nucleotide-binding oligomerization domain-like receptor, also NLR), or NACHT-LRR (NAIP, CIITA, Het-E-1, TLP1, LRR) family (18–21). NLR proteins contain three evolutionarily conserved domains: a variable N-terminal domain; a nucleotide binding domain; and a C-terminal LRR region. To date, >20 NLR

*Department of Microbiology and Immunology, †Curriculum in Genetics and Molecular Biology, ‡Lineberger Comprehensive Cancer Center, Department of Pathology, and §School of Dentistry Diagnostic Sciences and General Dentistry, University of North Carolina, Chapel Hill, NC 27599

Received for publication March 31, 2008. Accepted for publication December 10, 2008.

The costs of publication of this article were defrayed in part by the payment of page charges. This article must therefore be hereby marked *advertisement* in accordance with 18 U.S.C. Section 1734 solely to indicate this fact.

[1] This work was supported by National Institutes of Health Grants 1-R01-DE016326-01A1 and 1-U54-AI057157-03 (to J.P.-Y.T.).

[2] Address correspondence and reprint requests to Dr. Jenny Pan-Yun Ting, Lineberger Comprehensive Cancer Center, University of North Carolina, Chapel Hill, NC 27599. E-mail address: panyun@med.unc.edu

[3] Abbreviations used in this paper: NLR, nucleotide-binding domain leucine-rich repeat; LRR, leucine-rich repeat; NACHT, the NAIP, CIITA, HET-E, and TP1 domain; NALP3, the NACHT-, LRR-, PYD-containing protein; CARD, caspase recruitment domain; ASC, apoptotic speck protein containing a CARD; MOI, multiplicity of infection; Sh-, short hairpin-; PI, propidium iodide; TEM, transmission electron microscopy; PARP, poly(ADP-ribose) polymerase; Sh-CNTRL, control Sh-RNA with a mutated target ASC sequence; EV, empty vector.

www.jimmunol.org/cgi/doi/10.4049/jimmunol.0800909

family members have been identified in humans, and roles in immunity have been elucidated for several. One of the best-characterized family members is NLRP3 (formerly cryopyrin). Mutations in the *NLRP3* gene have been identified in a trio of autoinflammatory disorders, collectively named CAPS (*C*IAS1-*a*ssociated *p*eriodic *s*yndrome; Ref. 21). NLRP3 interacts with an adaptor molecule, apoptosis-associated speck-like protein containing a CARD (ASC), also known as TMS1 (22, 23). ASC is a small bipartite protein consisting of an N-terminal pyrin domain and a CARD). ASC and NLRP3, together with procaspase-1, form a multiprotein complex termed the inflammasome (21, 24, 25). When a cell encounters specific pathogens or host danger signals, it is believed that the pyrin domain of ASC interacts with the pyrin domain of NLRP3, whereas the CARD domain interacts with the CARD domain of procaspase-1 (25, 26). This leads to the activation of caspase-1 and subsequent maturation of pro-IL-1β to mature IL-1β for release.

In addition to IL-1β processing, NLRP3 and ASC mediate pathogen-induced cell death (27, 28). ASC was first isolated and characterized in monocytic HL60 cells undergoing apoptosis (22, 29). Overexpression of ASC causes mitochondrial-dependent apoptosis which can be blocked by dominant negative caspase-9 but not dominant negative caspase-8 (23). In nonhemopoietic cells, ASC has been demonstrated to be an adaptor of bax in p53-mediated apoptosis pathways (29). Macrophages derived from ASC-deficient mice have been shown to be resistant to cell death when exposed to *Francisella tularensis* (27). These authors speculated that macrophages undergo cell death when infected with *F. tularensis* as a last line of defense to prevent bacteria from replicating intracellularly. Another report shows that *Shigella flexneri* induces NLRP3- and ASC-dependent necrosis that results in the release of proinflammatory mediators such as HMGB1 (28). The nature of cell death is critical as necrotic cell death exacerbates local inflammation whereas apoptotic cells elicit minimal impact within the microenvironment. Because ASC and the inflammasome clearly play an important role in the cell death elicited by multiple human pathogens, we hypothesized that they might also be important in *P. gingivalis*-induced cell death mechanisms. In addition, because mechanisms of *P. gingivalis*-elicited cell death have not yet been clearly defined, we sought to characterize *P. gingivalis*-induced cell death in the context of the inflammasome.

The present study shows that *P. gingivalis* induces a necrotic-like cell death in THP1 cells and primary human macrophages and that ASC and NLRP3 are both important for *P. gingivalis*-induced cell death. This form of cell death is accompanied by the formation of a large ASC complex in dying cells, representing the first observation of an ASC speck aggregate in response to a microbial pathogen.

Materials and Methods

Cell culture and peripheral blood macrophage preparation

THP1 cells (American Type Cultue Collection; ATCC) were cultured in RPMI 1640 with 10% characterized FBS. Peripheral blood macrophages were isolated on buffy coats from healthy donors (American Red Cross). Primary macrophages were harvested by Ficoll-Hypaque gradients and seeded in 10 ml of RPMI 1640 containing 10% heat-inactivated FBS. Non-adherent cells were removed. Where indicated, cells were treated for 24–72 h with *P. gingivalis* strain A7436, *Escherichia coli* or *Salmonella typhi* at the indicated multiplicity of infection (MOI), with 0.1–1 μM staurosporine (Sigma-Aldrich), or with 0.01 or 0.1 μg/ml Ultrapure *P. gingivalis* LPS (InvivoGen). *P. gingivalis* LPS was purified from strain ATCC33277 (12) according to the manufacturer's instructions and would be expected to function as either a TLR2 or a TLR4 agonist (InvivoGen). ApoAlert VAD-fmk (pan-caspase inhibitor; 10 μM) or YVAD-cmk (caspase-1 inhibitor; both from BD Clontech) or 10 μg/ml IL-1 receptor antagonist Anakinra (Kineret; Amgen) was added 2 h before *P. gingivalis* where indicated.

Bacterial culture and viability assays

P. gingivalis strains A7436 was cultured anaerobically and *E. coli* strain DH5α aerobically as previously described (30). Bacteria were collected by centrifugation and resuspended in broth containing 20% glycerol. Frozen aliquots were stored at −80°C. The MOI of the inoculum was confirmed by plating serial dilutions of *P. gingivalis* anaerobically on either blood agar or Wilkins-Chalgren agar, and *E. coli* aerobically on Luria-Bertani agar. Counts are accurate within 1.5-fold. For viability assays, THP1 cells (control, ASC, and NLRP3 knockdowns) were washed three times and resuspended in antibiotic-free medium (RPMI 1640 and 10% FBS). Cells (10^6/ml) were seeded and exposed to various MOIs of *P. gingivalis* for 24, 48 and 72 h. After bacteria/cell interactions, total cultures (THP1 and *P. gingivalis*) were plated in serial dilution anaerobically in either blood agar or Wilkins-Chalgren agar. CFUs were counted, and CFUs per milliliter of total culture were calculated and estimated. At least three independent experiments were performed, and a representative experiment is shown.

Preparation of short hairpin (Sh-) RNA plasmids and cell lines for ASC and NLRP3 knockdown

Plasmids for expression of Sh-RNAs were made by inserting a histone H1 promoter, Sh-RNA, and termination sequence into a GFP-containing pHSPG retroviral shuttle vector as previously described (28, 30). The Sh-RNA target sequences are Sh-ASC #1-GCTCTTCAGTTTCACACCA; control Sh-RNA with a mutated target ASC sequence (Sh-CNTRL) – GC TCTTCctggcCACACCA; Sh-ASC #2-CCTGGAACTGGACCTGCAA; Sh-NLRP3 #1-GGATGAACCTGTTCCAAAA; and Sh-NLRP3 #2-AGAT GGAGTTGCTGTTTGA. IFN response was not activated by Sh-RNA as assessed by OAS1 expression (not shown).

Real-time PCR analysis

Preparation of RNA and cDNA was performed using RNeasy column purification and Moloney murine leukemia virus as previously described (30). Real-time PCR experiments were performed using an AB Prism 7700 thermocycler (Applied Biosystems) with 58°C annealing temperature. All values were normalized to 18S expression. Primer used are as follows. ASC: forward, AACCCAAGCAAGATGCGGAAG; reverse, TTAGGGCCTG GAGGAGCAAG. NLRP3: forward, ATGCCAGGAAGACAGCATTG; reverse, TCATCGAAGCCGTCCATGAG. 18S, forward, CGGCTACCAC ATCCAAGG; reverse, GCTGCTGGCACCAGACTT.

ELISA

Supernatants were assessed 18–24 h after stimulation using a human IL-1β ELISA set (BD Biosciences). Samples were assayed within linear range. All values represent averages plus SD of experiments performed in triplicate.

Cell death measurement

Bacteria induced cell death in THP1 cells was assessed by incubation of cells with medium containing Hoechst 33342 (10 μM) and propidium iodide (PI; 20 μM) for 10 min at 37°C. Results were visualized and imaged under a Zeiss fluorescent inverted microscope with a UV filter. Cell numbers ($\geq$2000 cells/field) were quantified by using Image J software (National Institutes of Health). Cell death is represented as a percentage of PI-positive cells (% PI-positive cells = (PI-positive cells/Hoechst 33342-positive cells) $\times$ 100). Quantification of *P. gingivalis* LPS-treated cells required a less stringent setting of intensity in Image J to accurately estimate the percentage of PI-positive cells due to the clumping of cells upon *P. gingivalis* LPS treatment. Results represent the average total of experiments performed in triplicate.

ASC Western analysis

Cell lysates of Sh-CNTRL and Sh-ASC were prepared as described previously (30). Immunoblots for ASC and GAPDH were performed using anti-ASC Ab (Axxora) and anti-GAPDH Ab (Santa Cruz Biotechnology). All results are representative of three independent experiments.

Poly(ADP-ribose) polymerase (PARP) cleavage assays

Cell lysates were prepared as described previously (28, 30). Immunoblots for PARP were performed using anti-PARP Ab (Santa Cruz Biotechnology). All results are representative of three independent experiments.

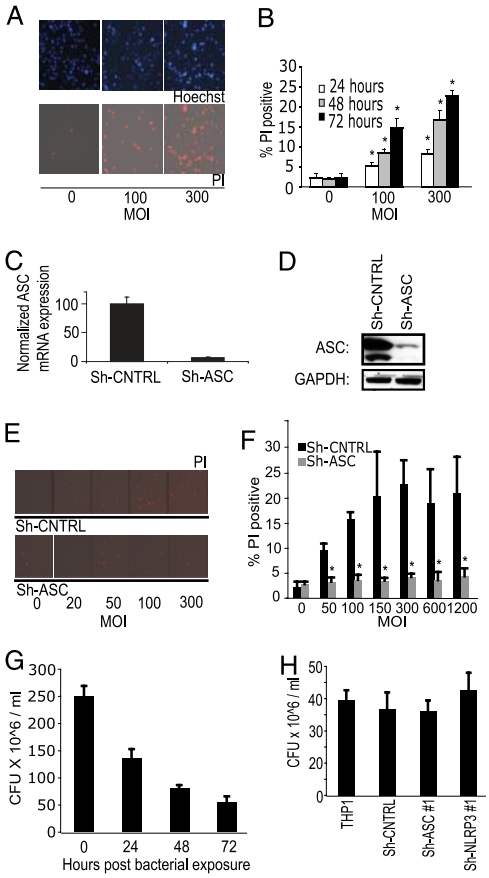

FIGURE 1. *P. gingivalis*-induced cell death is ASC dependent in THP1 monocytic cells. *A*, Visualization of *P. gingivalis*-induced cell death by PI staining. THP1 cells were exposed to *P. gingivalis* at MOIs of 0, 100, or 300 for 72 h and stained with Hoechst 33342 (blue) and PI (red). Hoechst stains all cells, whereas PI stains cells that lose membrane integrity while undergoing cell death. At least three independent experiments were performed. Each experiment was composed of triplicate wells per dose of *P. gingivalis* exposure. An image was taken per well, and a representative image is shown. *B*, Quantification of PI staining following a time course of *P. gingivalis* infection. THP1 cells were exposed to *P. gingivalis* at the indicated MOI for 24, 48, or 72 h. Cell death was evaluated by PI exclusion and quantified as percent PI positive using Image J computer software to count cells. Bars, SD of the mean for three independent experiments performed in triplicate. *, $p < 0.05$ when compared with untreated controls. *C*, Reduced ASC expression in ASC knockdown THP1 cells. ASC expression in Sh-ASC cells was measured by real-time PCR and was compared with expression in THP1 cells stably transfected with a specific control vector (Sh-CNTRL). Results represent average plus SD for triplicate samples. *D*, Reduced ASC expression in ASC knockdown THP1 cells. ASC expression in Sh-ASC cells was measured by Western analysis and was compared with expression in THP1 cells stably transfected with a specific control vector (Sh-CNTRL). GAPDH is shown as a loading control. Results are representative of three independent experiments. *E*, THP1 cells bearing an ASC Sh-RNA knockdown (Sh-ASC) or a control Sh-RNA containing a scrambled target site (Sh-CNTRL) were exposed to *P. gingivalis* for 72 h at the indicated MOI. Cell death was visualized by PI exclusion assay as described in *A*. At least three independent experiments were performed in triplicate. An image was taken for each well per dose, and a representative image is shown. *F*, Sh-CNTRL and Sh-ASC cells were treated with *P. gingivalis* at MOI of 0–1200 for 72 h. Cells were stained with PI following 72 h exposure to *P. gingivalis* and the percentage of PI-positive cells was quantified using Image J. Bars, SD of the mean for three independent experiments performed in triplicate. *, $p < 0.05$ when compared with Sh-CNTRL with respective *P. gingivalis* dose exposure. *G*, THP1 cells were exposed to *P. gingivalis* at MOI 300. *P. gingivalis* was recovered 0, 24, 48, and 72 h post-bacterial exposure from THP1 culture by plating by serial dilution, and CFU per milliliter was calculated. At least three independent experiments were performed in triplicate. A representative experiment is shown. Bars, SD of the mean of triplicate wells. *H*, THP1, Sh-CNTRL, Sh-ASC #1, and Sh-NLRP3 #1 were exposed to *P. gingivalis* at MOI 300. *P. gingivalis* was recovered 72 h post-bacterial exposure from THP1 culture by plating by serial dilution and CFU per milliliter was calculated. At least three independent experiments were performed in triplicate. A representative experiment is shown. Bar, SD of the mean of triplicate wells.

Transmission electron microscopy

Routine transmission electron microscopy (TEM) was conducted as described previously (28). For immunoelectron microscopy, cells were fixed in suspension with 4% paraformaldehyde, 0.15% glutaraldehyde, 0.15 M sodium phosphate for 1 h at room temperature. The cells were stained using an immunogold-silver protocol (31). A 1/250 dilution was used for the primary Ab (rabbit anti-ASC; Axxora) and a 1/100 dilution for the secondary Ab (donkey anti-rabbit IgG 0.8 nm immunogold (Aurion Netherlands; Electron Microscopy Sciences). Sections of 70 nm were cut, mounted on nickel grids, silver enhanced for 30 min, and stained with Reynolds' lead citrate. Samples were observed using a LEO EM910 transmission electron microscope operating at 80 kV (LEO Electron Microscopy). Digital images were acquired using a Gatan Orius SC1000 charge-coupled device digital camera and digital micrograph 3.11.0 (Gatan).

ASC aggregation speck visualization and quantification

Before immunofluorescent staining, THP1 cells or primary peripheral blood macrophages were washed three times in PBS and fixed in 100% methanol. Rabbit anti-human ASC (Axxora) was used to stain for endogenous ASC. Anti-rabbit Alexa Fluor 488 (Molecular Probes) was used as a secondary Ab. Background staining was controlled by staining cells using an isotype control Ab. Visualization of endogenous ASC was performed on a Zeiss LSM5 PASCAL confocal microscope. ASC specks were quantified as follows. The number of speck-containing cells was divided by total number of cells × 100 per field. At least 10 fields of ≥150 cells were blindly selected and counted per experiment, and the average and SD were calculated.

Overexpression of NLRP3 and disease-associated NLRP3 mutant R260W *in THP1 cells*

Adenovirus encoding NLRP3 *WT* and a disease-associated mutant *R260W* were transduced in THP1 cells at an MOI of 1 as previously described (28). Cells were assayed 9 h posttransduction.

Results

P. gingivalis *induces cell death in THP1 monocytic cells*

To determine whether *P. gingivalis* induces cell death in human monocytes/macrophages, we infected THP1 cells with *P. gingivalis* strain A7436 (32) and measured cell death using a PI exclusion assay. Cell death is reflected by the loss of membrane integrity and corresponding uptake of the fluorescent dye. A Hoechst 33342 stain was simultaneously used to reveal all cells in the sample. *P. gingivalis* induced a dose-dependent cell death in THP1 cells as visualized by increased PI staining (Fig. 1*A*). Results are quantified in Fig. 1*B*. In the absence of pathogen exposure, ~2–5% of cells were PI positive, indicating a low basal level of cell death. Exposure to *P. gingivalis* caused a reproducible and time-dependent increase in cell death. Exposing THP1 cells for 48 h caused 8–16% of cells to undergo cell death (Fig. 1*B*, gray bars), whereas exposure for 72 h caused 16–25% cell death (Fig. 1*B*, black bars). Viability assays demonstrate that *P. gingivalis* can still be recovered 24, 48, and 72 h after exposure to THP1 (Fig. 1*G*). These findings suggest that *P. gingivalis* can cause cell death as measured by PI exclusion staining and that some level of *P. gingivalis* remains viable in these cultures.

P. gingivalis*-induced cell death in THP1 cells is ASC and NLRP3 dependent*

ASC is a critical regulator of *P. gingivalis*-induced release of IL-1β and other cytokines in THP1 cells (30). To extend our findings, we tested whether *P. gingivalis*-induced cell death is ASC

dependent. Sh-RNA molecules were designed to promote the degradation of ASC mRNA (Sh-ASC). Sh-CNTRL was also prepared. Using retroviruses, these Sh-RNAs were stably incorporated into THP1 cells, resulting in ~90% reduction of ASC mRNA and protein (Ref. 30 and Fig. 1, *C* and *D*). We exposed Sh-ASC and Sh-CNTRL cells to *P. gingivalis* for 72 h and measured cell death levels in each cell line. Whereas Sh-CNTRL cells underwent significant levels of cell death after infection with 100 and 300 MOI of *P. gingivalis*, the level of cell death in Sh-ASC knockdown cells was greatly reduced (Fig. 1, *E* and *F*). The dose dependency of *P. gingivalis*-induced cell death reached a maximal level at ~150–300 bacteria per cell. However, even after Sh-ASC-containing cells were exposed for 72 h to 1200 *P. gingivalis* organisms per cell, little cell death was observed (Fig. 1*F*). These differences were not explained by differing levels of *P. gingivalis* viability because equivalent amounts of *P. gingivalis* were recovered from control and Sh-ASC cell cultures in a viability assay (Fig. 1*H*). These results indicate that ASC is essential for *P. gingivalis*-induced cell death in THP1 cells.

NLRP3 is known to interact with ASC within the inflammasome complex and is necessary for IL-1β release and cell death induced by multiple pathogens (28, 33–35). To determine whether NLRP3 is required for *P. gingivalis*-induced IL-1β and cell death, two independent Sh-RNAs specific for the *NLRP3* gene were stably expressed in THP1 cells, Sh-NLRP3 #1, and Sh-NLRP3 #2. Analysis by real-time PCR shows that *NLRP3* mRNA expression levels were reduced by 80% in Sh-NLRP3-containing cells as compared with control cells (Fig. 2*A*). NLRP3 protein also has been shown to be reduced by the Sh-RNA (28). Based on studies using multiple other types of bacterial pathogens, a reduction of *NLRP3* would be expected to reduce IL-1β production (28, 35). Indeed, levels of IL-1β induction were reduced in cells containing Sh-ASC, as well as both Sh-NLRP3 knockdown lines following infection with 50 MOI of *P. gingivalis* (Fig. 2*B*). These findings verify the functionality of the knockdown. Cytokine is induced at a shorter time course than cell death and upon infection with a lower dose of *P. gingivalis*, and it was therefore important for this study to test the knockdown in the context of a cell death assay. To determine whether NLRP3 is required for cell death induced by *P. gingivalis*, cells containing Sh-NLRP3 were exposed to *P. gingivalis* and assessed by PI exclusion assay (Fig. 2*C*). Cells with an empty vector (EV) underwent cell death in a dose-dependent manner; however, cells with Sh-NLRP3 did not undergo a significant increase in cell death, even when exposed to 300 MOI of *P. gingivalis* for 72 h. These results were verified using a panel of control cell lines and ASC and NLRP3 knockdown cell lines targeting two different sites for each gene (Fig. 2*D*). The use of two Sh-RNAs for each gene greatly reduces the likelihood that these results are due to the off-target effects of Sh-RNA. These findings indicate that *P. gingivalis*-induced cell death in THP1 cells is ASC and NLRP3 dependent.

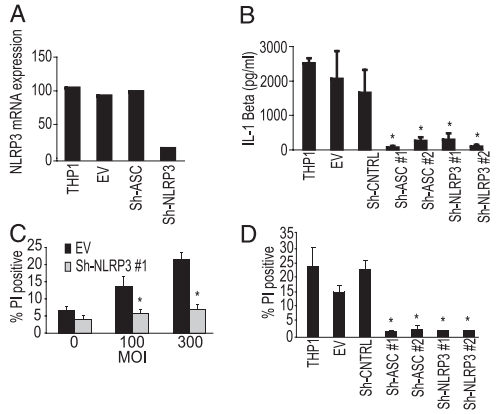

FIGURE 2. *P. gingivalis* induces NLRP3-dependent cell death. *A*, Reduced NLRP3 expression in NLRP3 knockdown THP1 cells. NLRP3 expression in Sh-NLRP3 cells was measured by real-time PCR and was compared with expression in nontransfected THP1 cells (THP1) and THP1 cells stably transfected with an empty vector (EV) or Sh-RNA against ASC (Sh-ASC #1). *B*, Reduced IL-1β induction in NLRP3 knockdown cells. Cells were exposed to *P. gingivalis* at MOI 50 for 24 h, and secreted IL-1β was measured by ELISA. Reduced IL-1β induction is shown for two ASC knockdown THP1 cell lines (Sh-ASC #1 and Sh-ASC #2), as well as two NLRP3 knockdown lines (Sh-NLRP3 #1 and Sh-NLRP3 #2). IL-1β induction in THP1 cells, THP1 cells expressing an EV, and THP1 cells expressing Sh-RNA with a scrambled target (Sh-CNTRL) were assayed as a control. Bars, SD of the mean for three independent experiments performed in triplicate. *, $p < 0.05$ when compared with Sh-CNTRL treated with *P. gingivalis*. *C*, Induction of cell death in control and Sh-NLRP3 cells. Control EV (■) and Sh-NLRP3 knockdown cells (▨) were exposed to *P. gingivalis* for 72 h at the indicated MOI. Cell death was evaluated by PI exclusion assay and quantified using Image J. Bars, SD of the mean for three independent experiments performed in triplicate. *, $p < 0.05$ when compared with EV with respective *P. gingivalis* dose exposure. *D*, Cell death induction for a panel of control and Sh-RNA knockdown cell lines. Cell death was measured for control lines THP1, EV, and Sh-CNTRL; for ASC knockdown lines, Sh-ASC #1 and Sh-ASC #2; and for NLRP3 knockdown lines, Sh-NLRP3 #1 and Sh-NLRP3 #2. Cell lines were exposed to *P. gingivalis* at an MOI of 300 for 72 h before PI staining and quantification by Image J. Bars, SD of the mean for three independent experiments performed in triplicate. *, $p < 0.05$ compared with Sh-CNTRL treated with *P. gingivalis*.

P. gingivalis *LPS induces an ASC- and NLRP3-dependent cell death in THP1 cells*

The immunostimulatory activity of *P. gingivalis* is thought to derive from conserved structural components including fimbriae and LPS within its cell wall. Unlike LPS from *E. coli* and many other Gram-negative bacteria, *P. gingivalis* LPS activates host cells through TLR2 and TLR4 (8, 10–12, 36). To determine whether *P. gingivalis* LPS induces ASC-dependent cell death, PI exclusion assays were repeated using two different concentrations of ultrapure *P. gingivalis* LPS (Fig. 3*A*). The *P. gingivalis* LPS is purified from strain ATCC33277 according to the method of Coats et al. (12) and should be composed of lipid A species that are both agonists of TLR2 and TLR4. THP1 cells treated with *P. gingivalis* LPS appeared to clump together, a phenomenon not observed in bacteria exposed cells. The clumping made it difficult to count individual cells; however, microscopic images (Fig. 3*A*) and quantitation using a less stringent Image J software setting (Fig. 3*B*) show that, similar to intact *P. gingivalis, P. gingivalis* LPS elicits cell death in THP1 cells, and this process is ASC and NLRP3 dependent. These findings suggest that the LPS moiety of the *P. gingivalis* has a biological activity similar to that of the whole bacterium in inducing cell death in THP1 cells through an ASC- and NLRP3-dependent mechanism.

ASC- and NLRP3-dependent cell death in THP1 cells is pathogen specific

To determine whether ASC and NLRP3 participate in cell death induced by an alternate Gram-negative bacteria, we exposed EV, Sh-ASC, and Sh-NLRP3 cells to *E. coli* and measured cell death (Fig. 3*C*). Ten MOI of *E. coli* induced more cell death than 100 MOI of *P. gingivalis* strain A7436, possibly due to the rapid growth of the bacteria and acute nature of infection as compared with *P. gingivalis.* Although these bacteria cannot be directly compared, results suggest that cell death was dependent on ASC and

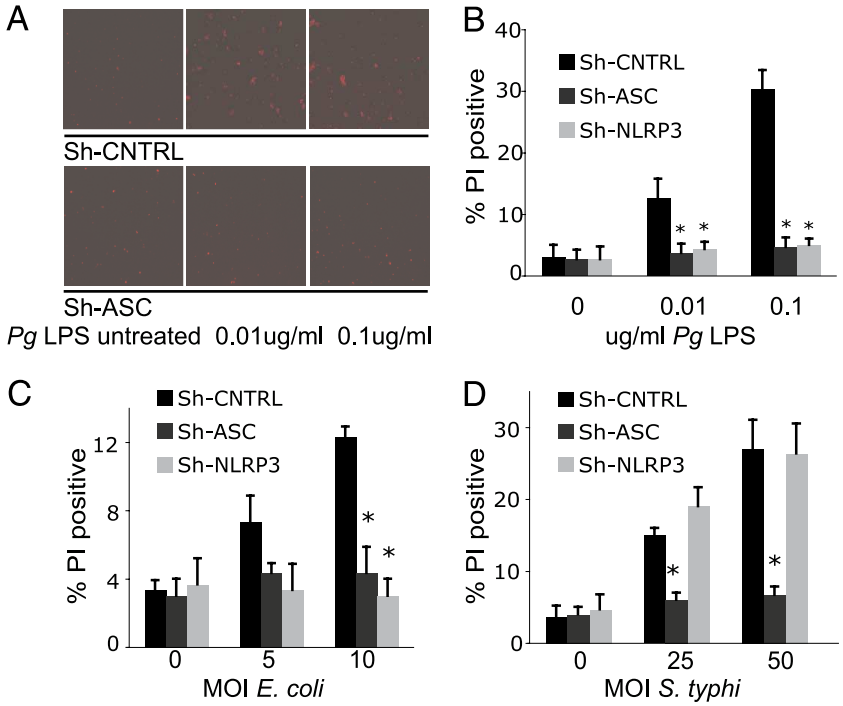

FIGURE 3. Bacteria-induced cell death is pathogen specific. *A*, Induction of cell death by *P. gingivalis* (*Pg*) LPS is ASC dependent. Sh-CNTRL and Sh-ASC cells were left untreated or were treated with 0.01 or 0.1 μg/ml *P. gingivalis* LPS for 24 h. Cell death was evaluated by PI exclusion assay. At least three independent experiments were performed in triplicate. An image was taken for each well per dose, and a representative image is shown. *B*, Sh-CNTRL, Sh-ASC, and Sh-NLRP3 cells were treated with 0, 0.01, or 0.1 μg/ml *P. gingivalis* LPS for 24 h. Cell death was evaluated by PI exclusion assay and quantified by Image J software. Results are the average plus SD of three independent experiments performed in triplicate wells. *C*, Induction of cell death in ASC and NLRP3 knockdown cells following infection with *E. coli*. EV, Sh-ASC, and Sh-NLRP3 cells were exposed to *E. coli* at MOIs of 5 and 10 for 24 h, and cell death was evaluated using PI exclusion assay and quantified using Image J. Bars, SD of the mean for three independent experiments. *, $p < 0.05$ compared with Sh-CNTRL with respective *E. coli* dose exposure. *D*, *Salmonella typhi* induces an ASC-dependent but NLRP3-independent cell death. THP1 cells Sh-CNTRL, Sh-ASC, and Sh-NLRP3 were treated with *Salmonella typhi* for 1 h at MOI 50. Cell death was evaluated using a PI exclusion assay and quantified using Image J. Bars, SD of the mean for three independent experiments. *, $p < 0.05$ when compared with Sh-CNTRL with respective *Salmonella. typhi* dose exposure.

NLRP3 for both pathogens. In contrast, previous reports and our data suggest that *F. tularensis* and *S. typhi*-induced cell death is ASC dependent but not NLRP3 dependent (Fig. 3*D*) (28, 34, 37). These results suggest that similar mechanisms may be involved in the induction of cell death in THP1 cells by *P. gingivalis* and *E. coli* and that dependency on ASC and NLRP3 may be pathogen specific. Further studies will be necessary to directly compare pathogens at a range of doses and times of infection, but these initial sets of studies could imply pathogen specificity.

P. gingivalis-*induced cell death in THP1 cells exhibits features consistent with necrosis*

The PI exclusion results suggest that THP1 cells exhibit a loss of cell membrane integrity after 72 h of *P. gingivalis* exposure. Data from other laboratories suggest that membrane permeabilization during necrotic-type cell death may function to alert the immune system to invading pathogens (38). To characterize the mechanisms of *P. gingivalis* in inducing cell death, we treated THP1 cells with 100 MOI of *P. gingivalis* strain A7436 for 72 h and examined cellular changes in morphology by TEM. As a control, cells were treated with staurosporine, a well-characterized apoptosis-inducing agent. Staurosporine induced features typical of apoptosis but did not cause a loss of membrane integrity (Fig. 4*Ai* and *Aii*). In contrast, Sh-CNTRL underwent a morphologically distinct form of cell death when exposed to *P. gingivalis*, as evidenced by the chromatin condensation and loss of cell membrane integrity (Fig. 4*Aiii*). These features are typical of necrosis occurring during inflammatory cell death. By comparison, Sh-ASC cells exposed to *Pg* did not exhibit features of apoptosis, nor did they exhibit the compromised membrane typical of necrotic cell death (Fig. 4*Aiv*). These findings suggest that THP1 cells exposed to *P. gingivalis* undergo ASC-dependent cell death with features morphologically consistent with necrosis. We were unable to demonstrate *P. gingivalis*-induced cell death using conventional apoptosis assays including TUNEL and DNA laddering. This further suggests that *P. gingivalis*-induced cell death is necrotic-like rather than apoptotic.

P. gingivalis *induces caspase and IL-1β-independent cell death*

Caspases have been well characterized in classical apoptotic pathways. Our data suggest that *P. gingivalis* induces a proinflammatory necrotic-like cell death rather than apoptosis. It is established that most apoptosis can be blocked by Z-VAD-fmk, a pan-caspase inhibitor. In addition, caspase-1 represents an additional component of the IL-1β inflammasome (21). We previously showed that pretreating THP1 cells with either Z-VAD or the caspase-1-specific inhibitor Y-VAD blocked *P. gingivalis* A7436-induced IL-1β (30). To determine whether caspases are involved in *P. gingivalis*-induced cell death, we tested whether *P. gingivalis*-induced cell death in THP1 cells could be blocked by pretreatment with Y-VAD and Z-VAD. Pretreatment of cells with 10 μM concentrations of either Y-VAD or Z-VAD did not prevent THP1 cells from undergoing cell death (Fig. 4*B*). To assess the role of IL-1β in *P. gingivalis*-induced cell death, cells were pretreated with Kineret, an IL-1β receptor antagonist. Kineret treatment failed to abrogate

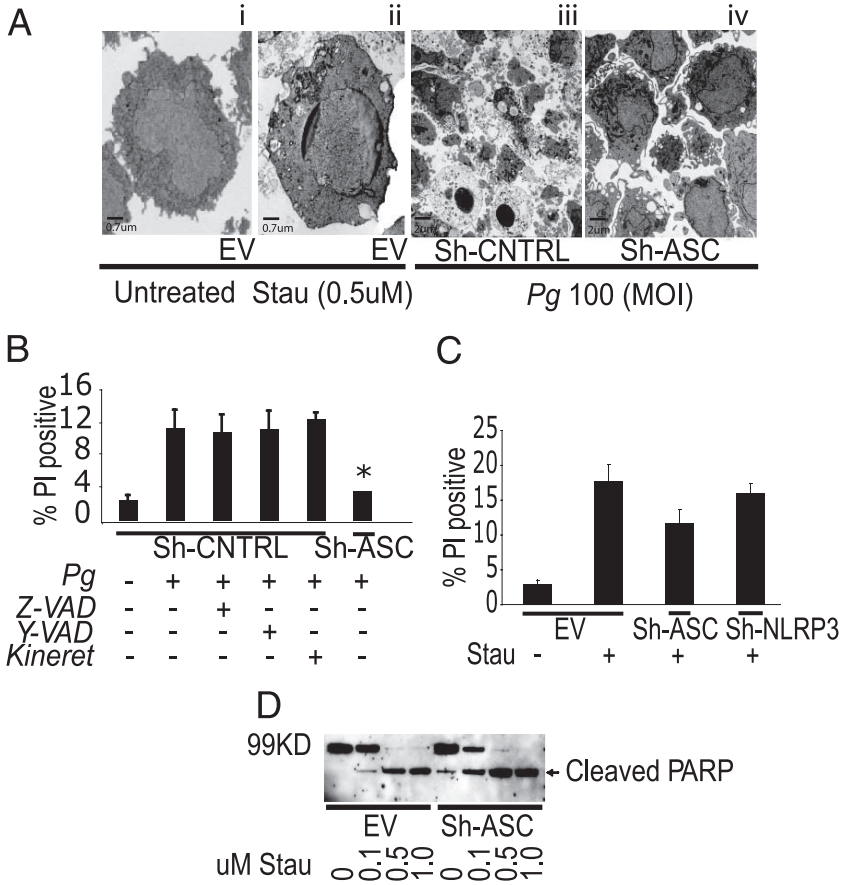

FIGURE 4. *P. gingivalis* (*Pg*) induces necrotic-like cell death. *A*, Characterization of *P. gingivalis*-induced cell death by TEM. TEM was performed on THP1 cells with an EV that were left untreated (*i*) or treated with 0.5 μM staurosporine (Stau; *ii*), on *P. gingivalis*-infected THP1 cells bearing a scrambled Sh-RNA target (Sh-CNTRL; *iii*) and on *P. gingivalis* -infected THP1 cells were bearing Sh-RNA against ASC (Sh-ASC; *iv*). *P. gingivalis* infections were at an MOI of 100 for 72 h. Two experiments were performed. Each experiment was comprised of duplicate wells per condition. At least 50 images were taken per condition and a representative image is shown. *B*, *P. gingivalis*-induced cell death is caspase and IL-1 independent. Cells were treated with *P. gingivalis* at an MOI of 300 for 48 h. Sh-CNTRL cells were pretreated with 10 μM pan-caspase inhibitor (Z-VAD), caspase-1-specific inhibitor (Y-VAD) or 10 μg/ml IL-1R antagonist (Kineret) 1 h before infection. Sh-ASC cells were infected with *P. gingivalis* in parallel. Cell death was evaluated using PI exclusion assay and quantified using Image J. Bars, SD of the mean for three independent experiments performed in triplicate. $*$, $p < 0.05$ compared with Sh-CNTRL with or without inhibitors exposed to *P. gingivalis*. *C*, Stauroporine-induced cell death is not ASC or NLRP3 dependent. THP1 cells with EV, Sh-ASC, or Sh-NLRP3 were treated with 0.5 μM staurosporine for 24 h. Cell death was evaluated using PI exclusion assay and quantified using Image J. Bars, SD of the mean for three independent experiments performed in triplicate. *D*, Staurosporine-induced PARP cleavage is not ASC dependent. THP1 cells with EV or Sh-ASC were treated with 0, 0.1, 0.5, and 1 μM staurosporine for 24 h, and PARP cleavage was evaluated by Western blotting. At least three independent experiments were performed. An image of a representative Western blotting experiment is shown.

cell death, suggesting that *P. gingivalis*-induced cell death is not mediated by IL-1β signaling. This suggests that caspases and IL-1β are not required for *P. gingivalis*-induced cell death.

To determine whether the role of ASC and NLRP3 is limited to inflammatory stimuli, we tested whether ASC and NLRP3 also play a role in staurosporine-induced cell death. Staurosporine efficiently induced cell death in control cells and in Sh-ASC- and Sh-NLRP3-containing cells (Fig. 4*C*). Differences in levels of cell death induction in the different cell lines are not statistically significant as determined by Student's *t* test. This result demonstrates the specificity of ASC and NLRP3 in cell death induced by bacteria.

PARP cleavage is a classical marker of apoptosis. To verify results from Fig. 4*C*, cells containing Sh-CNTRL and Sh-ASC were assessed for PARP cleavage following staurosporine treatment. Both groups of staurosporine-treated cells exhibited cleaved PARP in a dose-dependent manner (Fig. 4*D*). If anything, PARP levels were somewhat greater in Sh-ASC cells. Thus, ASC could potentially have some role in reducing excessive PARP cleavage but does not appear to be necessary for staurosporine-induced PARP cleavage.

P. gingivalis *induces ASC aggregate speck formation in THP1 cells*

ASC was originally characterized in the HL60 leukemic monocytic cell line where it aggregated into a cytosolic speck during cell death (22). However, speck formation has not been previously described in the context of microbial infection. We next investigated whether ASC aggregates in THP1 cells after exposure to *P. gingivalis*. THP1 cells were treated with *P. gingivalis* and stained with an Ab to endogenous ASC. Untreated cells were uniformly stained with ASC (Fig. 5*Aii*). In samples treated with *P. gingivalis*, two populations of cells were observed. In the first group, ASC aggregated into a single cytosolic speck, whereas the remaining population exhibited a uniform ASC distribution without a speck (Fig. 5, *Aiii* and *B*). ASC specks formed 24 h postinfection, and only one ASC speck was observed in each speck-containing cell. This latter observation is similar to the findings of Masumoto et al. (22), who

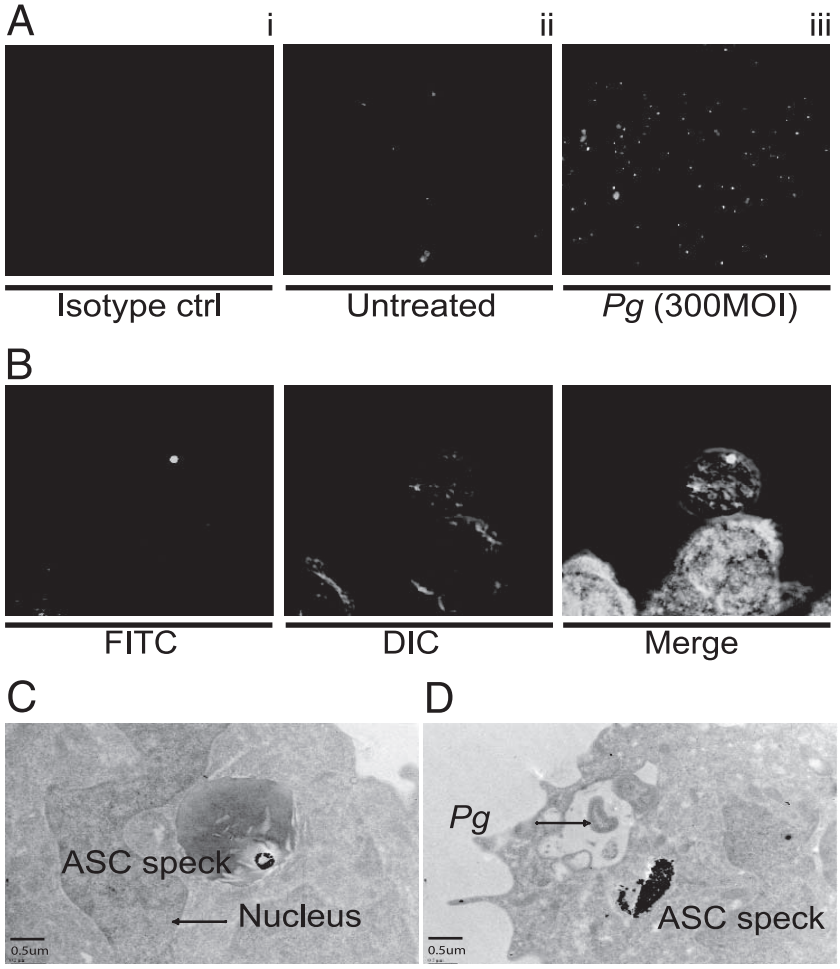

FIGURE 5. *P. gingivalis* induces ASC aggregation speck formation in THP1 cells. Endogenous characterization of ASC aggregation speck in THP1 cells. *Ai*, Untreated THP1 cells stained with rabbit isotype control Ab and secondary fluorochrome only; *Aii*, untreated cells stained with Ab against ASC and secondary fluorochrome; *Aiii*, THP1 cells exposed to *P. gingivalis* at an MOI of 300 for 24 h followed by staining with Ab against ASC and secondary fluorochrome. Cells were visualized by fluorescent microscopy using a ×20 lens. *B*, ×60 magnification of ASC speck formation in *P. gingivalis*-induced THP1 cells. Specks were visualized with a fluorescence filter (FITC) or differential interference contrast (DIC). A merged field is also shown. At least three independent experiments were performed per condition. At least 10 images were taken per condition, and representative images are shown. *C*, THP1 cells exposed to *P. gingivalis* at an MOI of 300 for 24 h followed by staining with TEM immunogold using an Ab against ASC. The position of the ASC speck is shown relative to the nucleus. *D*, TEM immunogold image showing an engulfed bacteria. Two independent experiments were performed in duplicate per condition. At least 50 images were taken per condition, and representative images are shown.

examined ASC speck formation caused by retinoic acid treatment. Our analyses also revealed that speck-containing cells appeared to be smaller and rounder than non-speck cells, possibly indicative of cell death. Cells containing the ASC specks were PI negative (data not shown). Because speck formation peaks before cell death as measured by the PI exclusion assay, this finding could suggest that ASC aggregates into specks before the loss of cell membrane integrity.

To define the morphology of ASC specks, TEM coupled with immunogold anti-ASC Ab labeling were used to examine the ASC speck in *P. gingivalis*-infected THP1 cells. The data indicate that gold-labeled ASC clusters into an amorphous mass of indiscernible structure (Fig. 5*C*). *P. gingivalis* can also be found in cells containing ASC specks, suggesting a correlation between bacterial engulfment and speck formation (Fig. 5*D*).

P. gingivalis-*induced ASC-aggregate speck formation in THP1 cells is NLRP3 dependent*

Because *Pg* induced cell death is both ASC and NLRP3 dependent (Figs. 1 and 2), we examined whether NLRP3 is required for *P. gingivalis*-induced ASC speck formation. ASC and NLRP3 knockdown cells were treated for 24 h with *P. gingivalis*, and at least 10 fields of ≥150 cells were randomly selected for quantification of specks. ASC specks were induced by *P. gingivalis* infection in control THP1 cells stably expressing an EV, but not in cells with either Sh-ASC or Sh-NLRP3 (Fig. 6*A*). This suggests that NLRP3 is required for both *P. gingivalis*-induced cell death and ASC speck formation. To further explore the role of NLRP3 in ASC speck formation, we transduced THP1 cells with recombinant

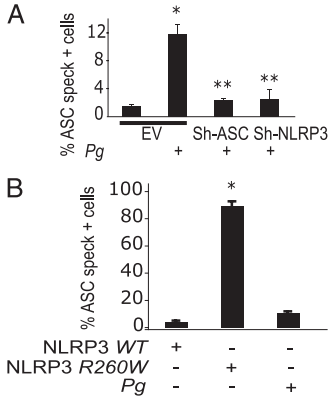

FIGURE 6. *P. gingivalis* (*Pg*)-induced ASC aggregation speck formation is NLRP3 dependent. *A*, Speck formation requires both ASC and NLRP3. THP1 cells with EV, Sh-ASC, and Sh-NLRP3 were exposed to *P. gingivalis* at an MOI of 100 for 24 h and stained for ASC specks. Cells were visualized using fluorescent microscopy, and the percent of cells containing ASC aggregation specks upon exposure to *P. gingivalis* was quantified. Bars, SD of the mean for three independent experiments performed in triplicate. *, $p < 0.05$ compared with untreated empty vector controls; **, $p < 0.05$ compared with *P. gingivalis*-treated EV controls. *B*, A disease-associated NLRP3 mutant induces speck formation. THP1 cells were transduced with adenovirus encoding a wild-type *NLRP3* gene or an NLRP3 disease-associated mutant, *R260W* or were exposed to *P. gingivalis* at an MOI of 100 for 24 h. ASC specks were visualized by immunostaining and fluorescent microscopy and were quantified as in *A*. Bars, SD of the mean for three independent experiments performed in triplicate. *, $p < 0.05$ for mutant NLRP3 when compared with cells treated with wild-type *NLRP3* gene.

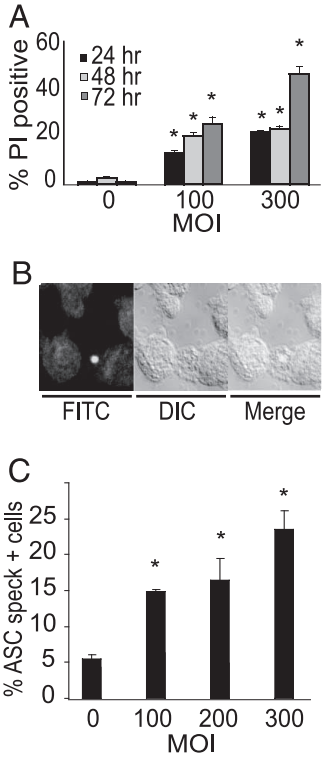

FIGURE 7. *P. gingivalis* induces cell death and ASC aggregation specks in human peripheral blood macrophages. *A*, Cell death induction in human peripheral blood macrophages following *P. gingivalis* treatment. Human peripheral blood macrophages were exposed to *P. gingivalis* at MOIs of 0, 100, or 300 for 24, 48, or 72 h as indicated. Cell death was evaluated using the PI exclusion assay and quantified using Image J. Bars, SD of the mean for three independent experiments performed in triplicate. *, $p < 0.05$ compared with untreated controls. *B*, Speck formation in human peripheral blood macrophages. Human peripheral blood macrophages exposed to *P. gingivalis* at an MOI of 100 for 24 h were stained for ASC, and specks were visualized using confocal microscopy (FITC). An image of the cells visualized by differential interference contrast (DIC) is also shown, as well as merged fields. Three independent experiments were performed. At least 10 images were taken per experiment, and representative images are shown. *C*, Quantification of specks in human peripheral blood macrophages. Human peripheral blood macrophages exposed to *P. gingivalis* at MOIs of 0–300 for 24 h were stained for ASC, and the percentage of cells containing ASC aggregation specks was quantified as in Fig. 6. Bars, SD of the mean for three independent experiments performed in triplicate. *, $p < 0.05$ compared with untreated control.

adenoviruses designed to express NLRP3 *WT* or a disease-associated, gain-of-function NLRP3 mutant, *R260W*. The NLRP3 *R260W* protein induces rapid necrotic-like cell death in THP1 cells, whereas the NLRP3 *WT* induces little or no cell death when overexpressed (28, 39). Consistent with these findings, NLRP3 *WT* did not induce significant speck formation, whereas NLRP3 *R260W* induced ASC speck formation in >90% of the THP1 cells as early as 9 h posttransduction (Fig. 6*B*). Specks were quantified at 9 h posttransduction since at the 24-h time point, NLRP3 *R260W* induced substantial cell death, and no cells were recoverable for ASC staining. The correlation between increased cell death and ASC speck formation with the gain-of-function NLRP3 mutant further supports a role for NLRP3 in ASC speck formation. Currently available anti-NLRP3 Abs, both commercial and those produced in our laboratory, are not optimal for microscopic identification of NLRP3 in the ASC specks; thus, we cannot directly resolve whether NLRP3 is contained within in the ASC specks.

P. gingivalis *induces cell death and ASC specks in primary human peripheral blood macrophages*

To extend these results to untransformed cells, we tested whether *P. gingivalis*-induced cell death and ASC aggregate speck formation occurs in primary human macrophages. *P. gingivalis* induced time- and dose-dependent cell death in primary human macrophages was measured by PI staining (Fig. 7*A*). When compared with THP1 cells, primary human macrophages exposed to *P. gingivalis* exhibited a higher level of cell death at the same dose and time of exposure (25–50% cell death). *P. gingivalis* also induced ASC aggregate speck formation in primary human macrophages (Fig. 7, *B* and *C*). These experiments demonstrate that *P. gingivalis* -induced cell death and ASC speck formation in THP1 cells are recapitulated in primary human cells.

Discussion

In this study, we investigated the role of NLRP3 and ASC in *P. gingivalis*-induced host cell death in a human monocytic cell line and primary human peripheral blood macrophages. We demonstrate that *P. gingivalis* induces a necrotic-like cell death requiring NLRP3 and ASC but not caspases (including caspase-1). *P. gingivalis*-infected cells exhibit characteristics morphologically indicative of necrosis, including a loss of membrane integrity and release of cellular contents. *P. gingivalis*-induced cell death is accompanied by ASC speck formation, which requires the presence of ASC and NLRP3. These findings are significant in that monocytic cells are crucial in the pathogenesis of periodontal disease (3). Importantly, *P. gingivalis*-induced necrosis and speck formation were observed in primary human macrophages. Although previous analyses have shown that either retinoic acid or the overexpression of ASC induces ASC speck formation (21, 22, 29), this is the first study to show that ASC speck formation occurs specifically in response to a microbial pathogen. The finding that ASC specks also occur in response to microbial pathogens indicates that specks are likely to be a biological phenomenon during the gingival disease process and potentially during infection in general. The ASC speck complex may represent an alternative target in elucidating the mechanisms of *P. gingivalis*-induced cell death as well as a potential target for therapy during microbial infection.

Our results suggest that *P. gingivalis*-induces a time- and dose-dependent cell death in THP1 cells and that a robust response occurs 72 h after infection with 300–600 bacteria/cell (Fig. 1). Similarly, the *P. gingivalis* strain FDC381 has been shown to require a MOI of 500-1000 to induce cell death (40). Our previous reports indicate that a MOI of 50 is sufficient to induce robust IL-1β release (30). It is difficult to estimate actual MOIs that occur during different stages of disease; however, it is generally acknowledged that MOI increases during disease progression and that cytokine release occurs before cell death. The different times and dosages leading to cytokine induction vs cell death suggest that cytokine release may be an early primary response, whereas cell death is a late response indicative of a higher bacteria load. Our results further demonstrate that *P. gingivalis*-induced cell death requires both ASC and NLRP3. *Shigella flexneri* also induces an ASC- and NLRP3-dependent macrophage cell death (28). Cell death induced by *F. tularensis* and by *Salmonella*, however, is ASC dependent but not NLRP3 dependent, suggesting specificity of pathogen-NLR pairing in host response (28, 34, 37).

We have shown that *P. gingivalis*-induced cell death is caspase independent. This finding suggests that the cell death process does not involve the formation of a conventional IL-1β inflammasome. Caspase-1 is a core component of the inflammasome and is required for IL-1β activation (25). Therefore, different mechanisms

may underlie cytokine activation and cell death. Further studies will be necessary to determine the nature of the protein complex regulating microbial pathogen-induced death.

Recently, Fernandes-Alnemri et al. (41) reported that proinflammatory stimuli such as LPS and monosodium urate induce ASC speck formation in THP1 cells in a caspase-1-dependent manner. Others have described a type of caspase-1-dependent cell death termed pyroptosis in *Salmonella*-infected macrophages that is characterized by cell swelling and osmotic lysis (42). In contrast, the biochemical and morphological features of *P. gingivalis*-induced cell death are consistent with pyronecrosis, a caspase-1-independent cell death pathway also activated by *Shigella flexneri* and *Campylobacter jejuni* (28, 43). However, overexpression studies have associated ASC with apoptosis (23, 29), and *F. tularensis* induces apoptotic ASC-dependent macrophage death in mice (27). Thus, it is reasonable to hypothesize that pathogens can induce both apoptotic and nonapoptotic host cell death, and ASC may serve a role in either type of cell death depending on the specific stimulation, the state of the cell, or other unknown factors.

The two-step release of proinflammatory cytokine IL-1β has been proposed by several studies (19, 35, 44). This represents a synergistic activation of TLR and NLR signaling pathways. First, bacteria and/or their cellular components activate a TLR/MyD88-dependent NF-κB signaling, thereby making pro-IL-1β available for release. The concurrent activation of the inflammasome via the NLR/ASC/caspase-1 axis then leads to cleavage and release of mature IL-1β to awaken the local immune response. TLRs are also critical for other cytokines such as TNF-α, IL-6, and IL-8. Pathogen-induced monocytic/macrophage necrotic-like cell death may represent an alternative or added approach to activate the immune system. In addition to the release of amplified levels of proinflammatory cytokines, the release of cellular contents by monocytes and macrophages during necrosis may send out an amplified host danger signal to alert the immune system to invading microorganisms (28). From this standpoint, it would be strategic for immune cells at the site of bacterial invasion to undergo necrosis and to release inflammatory mediators including cytokines and HMGB1 (45) to activate/recruit other inflammatory cells to aid in resolving an infection. Necrotic cell death is also known to propagate and exacerbate an inflammatory response. Future studies using an in vivo mouse model of *P. gingivalis* challenge should provide insights on whether the disruption of this NLRP3-ASC axis can alter periodontal disease pathogenesis and disease outcome.

P. gingivalis-induced cell death is accompanied by endogenous formation of ASC specks in monocytic cells following bacteria exposure, representing the first demonstration of endogenous ASC speck formation in response to a pathogen. Although ASC has a well-established role in cell death, far less is known about the protein complex that mediates ASC/NLRP3-dependent cell death or whether the ASC speck might represent a platform for formation of a death complex. Because cell death and speck formation are ablated in ASC and NLRP3 knockdown cells (Figs. 2 and 6*A*), NLRP3 appears to function in concert with ASC to cause death and speck formation.

In summary, our data indicate that NLRP3 and ASC are central in *P. gingivalis*-induced cell death and cytokine release. The necrotic-like nature of *P. gingivalis*-induced cell death in monocytes/macrophages may suggest a potential cellular host mechanism to combat infection. The critical roles of NLRP3 and ASC in macrophage cell death and ASC speck formation provide a first step in elucidating potential mechanisms of macrophage defense against *P. gingivalis*. The formation of ASC specks could serve as a novel molecular platform that fosters pathogen-induced cell death. These findings and future studies should lead to a better understanding of bacterial-induced periodontitis and could contribute to the design of better therapeutics.

Disclosures

The authors have no financial conflict of interest.

References

1. Southerland, J. H., G. W. Taylor, K. Moss, J. D. Beck, and S. Offenbacher. 2006. Commonality in chronic inflammatory diseases: periodontitis, diabetes, and coronary artery disease. *Periodontol. 2000* 40: 130–143.
2. Offenbacher, S., and J. D. Beck. 2005. A perspective on the potential cardioprotective benefits of periodontal therapy. *Am. Heart J.* 149: 950–954.
3. Zhou, Q., T. Desta, M. Fenton, D. T. Graves, and S. Amar. 2005. Cytokine profiling of macrophages exposed to *Porphyromonas gingivalis*, its lipopolysaccharide, or its FimA protein. *Infect. Immun.* 73: 935–943.
4. Graves, D. 2008. Cytokines that promote periodontal tissue destruction. *J. Periodontol.* 79: 1585–1591.
5. Steinberg, T., B. Dannewitz, P. Tomakidi, J. D. Hoheisel, E. Mussig, A. Kohl, and M. Nees. 2006. Analysis of interleukin-1β-modulated mRNA gene transcription in human gingival keratinocytes by epithelia-specific cDNA microarrays. *J. Periodontal Res.* 41: 426–446.
6. Palmqvist, P., P. Lundberg, I. Lundgren, L. Hanstrom, and U. H. Lerner. 2008. IL-1β and TNF-α regulate IL-6-type cytokines in gingival fibroblasts. *J. Dent. Res.* 87: 558–563.
7. Gamonal, J., A. Acevedo, A. Bascones, O. Jorge, and A. Silva. 2000. Levels of interleukin-1β, -8, and -10 and RANTES in gingival crevicular fluid and cell populations in adult periodontitis patients and the effect of periodontal treatment. *J.Periodontol.* 71: 1535–1545.
8. Wang, M., M. A. Shakhatreh, D. James, S. Liang, S. Nishiyama, F. Yoshimura, D. R. Demuth, and G. Hajishengallis. 2007. Fimbrial proteins of porphyromonas gingivalis mediate in vivo virulence and exploit TLR2 and complement receptor 3 to persist in macrophages. *J. Immunol.* 179: 2349–2358.
9. Hashimoto, M., Y. Asai, and T. Ogawa. 2004. Separation and structural analysis of lipoprotein in a lipopolysaccharide preparation from *Porphyromonas gingivalis*. *Int. Immunol.* 16: 1431–1437.
10. Bainbridge, B. W., S. R. Coats, and R. P. Darveau. 2002. *Porphyromonas gingivalis* lipopolysaccharide displays functionally diverse interactions with the innate host defense system. *Ann. Periodontol.* 7: 29–37.
11. Al-Qutub, M. N., P. H. Braham, L. M. Karimi-Naser, X. Liu, C. A. Genco, and R. P. Darveau. 2006. Hemin-dependent modulation of the lipid A structure of *Porphyromonas gingivalis* lipopolysaccharide. *Infect. Immun.* 74: 4474–4485.
12. Coats, S. R., R. A. Reife, B. W. Bainbridge, T. T. Pham, and R. P. Darveau. 2003. *Porphyromonas gingivalis* lipopolysaccharide antagonizes *Escherichia coli* lipopolysaccharide at Toll-like receptor 4 in human endothelial cells. *Infect. Immun.* 71: 6799–6807.
13. Reife, R. A., S. R. Coats, M. Al-Qutub, D. M. Dixon, P. A. Braham, R. J. Billharz, W. N. Howald, and R. P. Darveau. 2006. *Porphyromonas gingivalis* lipopolysaccharide lipid A heterogeneity: differential activities of tetra- and penta-acylated lipid A structures on E-selectin expression and TLR4 recognition. *Cell Microbiol.* 8: 857–868.
14. Hajishengallis, G., M. Wang, S. Liang, M. Triantafilou, and K. Triantafilou. 2008. Pathogen induction of CXCR4/TLR2 cross-talk impairs host defense function. *Proc. Natl. Acad. Sci. USA* 105: 13532–13537.
15. Gibson, F. C., 3rd, C. Hong, H. H. Chou, H. Yumoto, J. Chen, E. Lien, J. Wong, and C. A. Genco. 2004. Innate immune recognition of invasive bacteria accelerates atherosclerosis in apolipoprotein E-deficient mice. *Circulation* 109: 2801–2806.
16. Burns, E., G. Bachrach, L. Shapira, and G. Nussbaum. 2006. Cutting edge: TLR2 is required for the innate response to *Porphyromonas gingivalis*: activation leads to bacterial persistence and TLR2 deficiency attenuates induced alveolar bone resorption. *J. Immunol.* 177: 8296–8300.
17. Ting, J. P., R. C. Lovering, E. S. Alnemri, J. Bertin, J. M. Boss, B. K. Davis, R. A. Flavell, S. E. Girardin, A. Godzik, J. A. Harton, et al. 2008. The NLR gene family: a standard nomenclature. *Immunity* 28: 285–287.
18. Franchi, L., J. H. Park, M. H. Shaw, N. Marina-Garcia, G. Chen, Y. G. Kim, and G. Nunez. 2008. Intracellular NOD-like receptors in innate immunity, infection and disease. *Cell Microbiol.* 10: 1–8.
19. Mariathasan, S. 2007. ASC, Ipaf and cryopyrin/Nalp3: bona fide intracellular adapters of the caspase-1 inflammasome. *Microbes Infect.* 9: 664–671.
20. McDermott, M. F., and J. Tschopp. 2007. From inflammasomes to fevers, crystals and hypertension: how basic research explains inflammatory diseases. *Trends Mol. Med.* 13: 381–388.
21. Ting, J. P., D. L. Kastner, and H. M. Hoffman. 2006. CATERPILLERs, pyrin and hereditary immunological disorders. *Nat. Rev. Immunol.* 6: 183–195.
22. Masumoto, J., S. Taniguchi, K. Ayukawa, H. Sarvotham, T. Kishino, N. Niikawa, E. Hidaka, T. Katsuyama, T. Higuchi, and J. Sagara. 1999. ASC, a novel 22-kDa protein, aggregates during apoptosis of human promyelocytic leukemia HL-60 cells. *J. Biol. Chem.* 274: 33835–33838.
23. McConnell, B. B., and P. M. Vertino. 2000. Activation of a caspase-9-mediated apoptotic pathway by subcellular redistribution of the novel caspase recruitment domain protein TMS1. *Cancer Res.* 60: 6243–6247.
24. Petrilli, V., S. Papin, and J. Tschopp. 2005. The inflammasome. *Curr. Biol.* 15: R581.

25. Martinon, F., K. Burns, and J. Tschopp. 2002. The inflammasome: a molecular platform triggering activation of inflammatory caspases and processing of proIL-β. *Mol. Cell.* 10: 417–426.
26. Srinivasula, S. M., J. L. Poyet, M. Razmara, P. Datta, Z. Zhang, and E. S. Alnemri. 2002. The PYRIN-CARD protein ASC is an activating adaptor for caspase-1. *J. Biol. Chem.* 277: 21119–21122.
27. Mariathasan, S., D. S. Weiss, V. M. Dixit, and D. M. Monack. 2005. Innate immunity against *Francisella tularensis* is dependent on the ASC/caspase-1 axis. *J. Exp. Med.* 202: 1043–1049.
28. Willingham, S. B., D. T. Bergstralh, W. O'Connor, A. C. Morrison, D. J. Taxman, J. A. Duncan, S. Barnoy, M. M. Venkatesan, R. A. Flavell, M. Deshmukh, et al. 2007. Microbial pathogen-induced necrotic cell death mediated by the inflammasome components CIAS1/cryopyrin/NLRP3 and ASC. *Cell Host Microbes* 2: 147–159.
29. Ohtsuka, T., H. Ryu, Y. A. Minamishima, S. Macip, J. Sagara, K. I. Nakayama, S. A. Aaronson, and S. W. Lee. 2004. ASC is a Bax adaptor and regulates the p53-Bax mitochondrial apoptosis pathway. *Nat. Cell Biol.* 6: 121–128.
30. Taxman, D. J., J. Zhang, C. Champagne, D. T. Bergstralh, H. A. Iocca, J. D. Lich, and J. P. Ting. 2006. Cutting edge: ASC mediates the induction of multiple cytokines by *Porphyromonas gingivalis* via caspase-1-dependent and -independent pathways. *J. Immunol.* 177: 4252–4256.
31. Yi, H., J. Leunissen, G. Shi, C. Gutekunst, and S. Hersch. 2001. A novel procedure for pre-embedding double immunogold-silver labeling at the ultrastructural level. *J. Histochem. Cytochem.* 49: 279–284.
32. Genco, C. A., C. W. Cutler, D. Kapczynski, K. Maloney, and R. R. Arnold. 1991. A novel mouse model to study the virulence of and host response to *Porphyromonas* (*Bacteroides*) *gingivalis*. *Infect. Immun.* 59: 1255–1263.
33. Kanneganti, T. D., M. Lamkanfi, Y. G. Kim, G. Chen, J. H. Park, L. Franchi, P. Vandenabeele, and G. Nunez. 2007. Pannexin-1-mediated recognition of bacterial molecules activates the cryopyrin inflammasome independent of Toll-like receptor signaling. *Immunity* 26: 433–443.
34. Mariathasan, S., D. S. Weiss, K. Newton, J. McBride, K. O'Rourke, M. Roose-Girma, W. P. Lee, Y. Weinrauch, D. M. Monack, and V. M. Dixit. 2006. Cryopyrin activates the inflammasome in response to toxins and ATP. *Nature* 440: 228–232.
35. Sutterwala, F. S., Y. Ogura, M. Szczepanik, M. Lara-Tejero, G. S. Lichtenberger, E. P. Grant, J. Bertin, A. J. Coyle, J. E. Galan, P. W. Askenase, and R. A. Flavell. 2006. Critical role for NALP3/CIAS1/Cryopyrin in innate and adaptive immunity through its regulation of caspase-1. *Immunity* 24: 317–327.
36. Martin, M., J. Katz, S. N. Vogel, and S. M. Michalek. 2001. Differential induction of endotoxin tolerance by lipopolysaccharides derived from *Porphyromonas gingivalis* and *Escherichia coli*. *J. Immunol.* 167: 5278–5285.
37. Mariathasan, S., K. Newton, D. M. Monack, D. Vucic, D. M. French, W. P. Lee, M. Roose-Girma, S. Erickson, and V. M. Dixit. 2004. Differential activation of the inflammasome by caspase-1 adaptors ASC and Ipaf. *Nature* 430: 213–218.
38. Fink, S. L., and B. T. Cookson. 2005. Apoptosis, pyroptosis, and necrosis: mechanistic description of dead and dying eukaryotic cells. *Infect. Immun.* 73: 1907–1916.
39. Fujisawa, A., N. Kambe, M. Saito, R. Nishikomori, H. Tanizaki, N. Kanazawa, S. Adachi, T. Heike, J. Sagara, T. Suda, et al. 2007. Disease-associated mutations in CIAS1 induce cathepsin B-dependent rapid cell death of human THP-1 monocytic cells. *Blood* 109: 2903–2911.
40. Roth, G. A., H. J. Ankersmit, V. B. Brown, P. N. Papapanou, A. M. Schmidt, and E. Lalla. 2007. *Porphyromonas gingivalis* infection and cell death in human aortic endothelial cells. *FEMS Microb. Lett.* 272: 106–113.
41. Fernandes-Alnemri, T., J. Wu, J. W. Yu, P. Datta, B. Miller, W. Jankowski, S. Rosenberg, J. Zhang, and E. S. Alnemri. 2007. The pyroptosome: a supramolecular assembly of ASC dimers mediating inflammatory cell death via caspase-1 activation. *Cell Death Differ.* 14: 1590–1604.
42. Fink, S. L., and B. T. Cookson. 2006. Caspase-1-dependent pore formation during pyroptosis leads to osmotic lysis of infected host macrophages. *Cell Microbiol.* 8: 1812–1825.
43. Siegesmund, A. M., M. E. Konkel, J. D. Klena, and P. F. Mixter. 2004. *Campylobacter jejuni* infection of differentiated THP-1 macrophages results in interleukin 1β release and caspase-1-independent apoptosis. *Microbiology* 150: 561–569.
44. Lich, J. D., J. C. Arthur, and J. P. Ting. 2006. Cryopyrin: in from the cold. *Immunity* 24: 241–243.
45. El Mezayen, R., M. El Gazzar, M. C. Seeds, C. E. McCall, S. C. Dreskin, and M. R. Nicolls. 2007. Endogenous signals released from necrotic cells augment inflammatory responses to bacterial endotoxin. *Immunol. Lett.* 111: 36–44.